Article Chinese Science Bulletin

SPECIAL TOPIC October 2013 Vol.58 No.28-29: 3460–3466
Coseismic Deformation and Rupture Processes of the 2013 Lushan Earthquake doi: 10.1007/s11434-013-5998-5

Preliminary results pertaining to coseismic displacement and preseismic strain accumulation of the Lushan M_S7.0 earthquake, as reflected by GPS surveying

WU YanQiang[1], JIANG ZaiSen[1*], WANG Min[2], CHE Shi[3], LIAO Hua[4], LI Qiang[5], LI Peng[1], YANG YongLin[4], XIANG HePing[4], SHAO ZhiGang[1], WANG WuXing[1], WEI WenXin[1] & LIU XiaoXia[1]

[1] *CEA Key Laboratory of Earthquake Prediction (Institute of Earthquake Science), China Earthquake Administration, Beijing 100036, China;*
[2] *State Key Laboratory of Earthquake Dynamics, Institute of Geology, China Earthquake Administration, Beijing 100029, China;*
[3] *China Earthquake Administration, Beijing 100036, China;*
[4] *Earthquake Administration of Sichuan Province, Chengdu 610041, China;*
[5] *National Earthquake Infrastructure Service, China Earthquake Administration, Beijing 100036, China*

Received May 30, 2013; accepted June 25, 2013; published online July 18, 2013

This paper presents the coseismic displacement and preseismic deformation fields of the Lushan M_S7.0 earthquake that occurred on April 20, 2013. The results are based on GPS observations along the Longmenshan fault and within its vicinity. The coseismic displacement and preseismic GPS results indicate that in the strain release of this earthquake, the thrust rupture is dominant and the laevorotation movement is secondary. Furthermore, we infer that any possible the rupture does not reach the earth's surface, and the seismogenic fault is most likely one fault to the east of the Guanxian-Anxian fault. Some detailed results are obtainable. (1) The southern segment of the Longmenshan fault is locked preceding the Lushan earthquake. After the Wenchuan earthquake, the strain accumulation rate in the southeast direction accelerates in the epicenter of the Lushan earthquake, and the angle between the principal compressional strain and the seismogenic fault indicates that a sinistral deformation background in the direction of the seismogenic fault precedes the Lushan earthquake. Therefore, it is evident that the Wenchuan M_S8.0 earthquake accelerated the pregnancy of the Lushan earthquake. (2) The coseismic displacements reflected by GPS data are mainly located in a region that is 230 km (NW direction) × 100 km (SW direction), and coseismic displacements larger than 10 mm lie predominantly in a 100-km region (NW direction). (3) On a large scale, the coseismic displacement shows thrust characteristics, but the associated values are remarkably small in the near field (within 70 km) of the earthquake fault. Meanwhile, the thrust movement in this 70-km region does not correspond with the attenuation characteristics of the strain release, indicating that the rupture of this earthquake does not reach the earth's surface. (4) The laevorotation movements are remarkable in the 50-km region, which is located in the hanging wall that is close to the earthquake fault, and the corresponding values in this case correlate with the attenuation characteristics of the strain release.

Lushan earthquake, Longmenshan fault zone, strain accumulation status, continuous GPS surveying, coseismic displacement fields

Citation: Wu Y Q, Jiang Z S, Wang M, et al. Preliminary results pertaining to coseismic displacement and preseismic strain accumulation of the Lushan M_S7.0 earthquake, as reflected by GPS surveying. Chin Sci Bull, 2013, 58: 3460–3466, doi: 10.1007/s11434-013-5998-5

The epicenter of the Lushan M_S7.0 earthquake that occurred on April 20, 2013 is 103.0°E, 30.3°N, and the depth of the hypocenter is 13 km (http://www.csi.ac.cn). Focal-mechanism solutions show that this earthquake is a typical thrust event, and the seismogenic fault belongs to the southern segment of the Longmenshan Fault Zone (LFZ). Since this earthquake, few surface ruptures have been found [1], and the inversion results of this earthquake's rupture process

*Corresponding author (email: jiangzaisen@126.com)

indicate that the rupture does not reach the surface to any significant extent [2]. As a result, the distribution of the coseismic displacement may be more unusual, which would play an important role in determining the seismogenic fault, analyzing the strain release features and researching other geodynamics issues.

We first review the judgment process regarding the locking status of the southern segment of the LFZ based on the preliminary coseismic displacement distribution of the Wenchuan earthquake. Subsequently, we analyze the deformation characteristics before the Lushan earthquake using campaign GPS data. Finally, the coseismic displacement produced by the Lushan M_S7.0 earthquake is presented according to the combined solutions of continuous GPS surveying across the seismogenic fault. The GPS data are collected from the scientific-investigation GPS stations, the permanent GPS stations of the project Tectonic and Environmental Observation Network in China (TEONEC) and the continuous CORS GPS stations of the Earthquake Administration of Sichuan Province [3]. These results provide data that are fundamental to understanding the mechanics of the Lushan earthquake.

1 Review of the GPS monitoring process of the Lushan earthquake

The Lushan Earthquake has been recorded by the temporary continuous GPS network in the southern segment of the LFZ, which was set up by the Institute of Earthquake Science, China Earthquake Administration (CEA), after the Wenchuan earthquake. This GPS network was established based on judgments regarding the existence of locking faults in the southern segment of the LFZ. Thus, we review the establishment and monitoring process of this GPS network.

The preliminary results obtained in June 2008 of the coseismic displacement of the Wenchuan earthquake showed remarkable differences between the two GPS profiles located on the footwall across the middle-northern and southern segments of the LFZ. In particular, the profile across the middle-northern segment of the LFZ showed a typical attenuation characteristic that is associated with fault thrust and large-amplitude strain release (Figure 1(a)), while the profile across the southern segment of the LFZ illustrated a continuous extrusion-deformation distribution and indicated that this segment was still in locked status (Figure 1(b)). In addition, the time series of the QLAI station located at the east side and close to the southern segment of the LFZ clearly behaved differently from other stations on the same side. This station moved to the east quickly, in contrast to the western movement of other stations after the Wenchuan earthquake, but it showed a remarkable western movement when the Wenchuan earthquake occurred. The eastern movement of the QLAI station demonstrated that the accelerated eastern movement of the Bayan Har block caused by

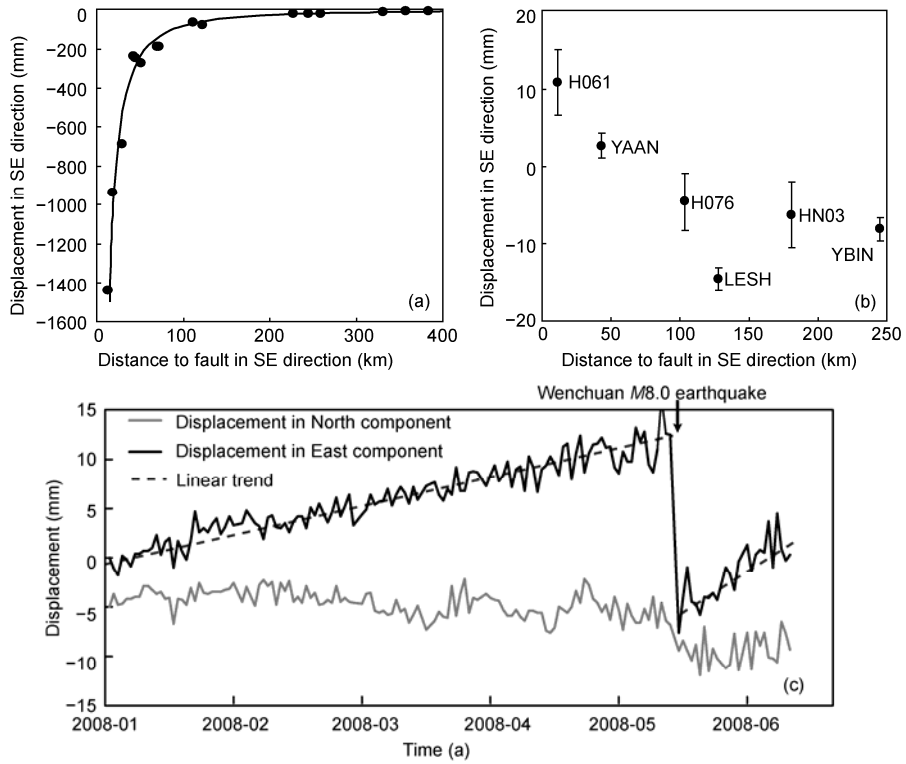

Figure 1 Influence of the Wenchuan M_S8.0 earthquake on surface displacement. (a) Horizontal displacement in the southeastern direction perpendicular to the middle segment of the LFZ; (b) horizontal displacement in the southeastern direction perpendicular to the southern segment of the LFZ; (c) horizontal displacement time series of the QLAI station.

the Wenchuan earthquake can transfer and affect the GPS sites located at the east side of the southern segment of the LFZ, thereby indicating that the southern segment of the LFZ was still in locked status after the Wenchuan earthquake.

The coseismic slip difference between fault segments caused by the Wenchuan earthquake, the geological investigation and digital seismology inversion results indicated that the southern segment of the LFZ had a risk of strong earthquakes. Especially, the inversion results of the rupture process indicated that the southern segment of the LFZ did not rupture. The team of Academician CHEN Yuntai suggested that this segment had an earthquake deficit region (http://www.csi.ac.cn/sichuan/sichuan080512_cs2.htm) and then warned of the risk of sudden great aftershocks in the future (http://focus.scol.com.cn/zgsz/20080523/2008523191636.htm). With the support of the Monitoring and Prediction Department (CEA), the Institute of Earthquake Science (CEA) set up a continuous GPS network in this region and entrusted the Institute of Surveying Engineering (Earthquake Administration of Sichuan Province) with building and routine maintenance. This network contains 10 continuous GPS sites that utilize Trimble NetRS instruments for geodesy. In the surveying process, the GPS receivers, data transmission equipment and power supply equipment are all positioned in the localities' family, and the GPS data are transmitted on regular days. This network has been supported for 6 months by the scientific investigations project of the Wenchuan earthquake. From the GPS results obtained during these 6 months, we found that the deformation rate of short baselines across the fault was small, but the deformation rate of long baselines was large. This result showed that the fault was still in locked status and that the strain loading rate was faster than before, indicating a high risk of earthquakes on the southern segment of the LFZ. Consequently, our research projects have continued to support the operation of this GPS network from 2009 to the present.

2 Crustal deformation characteristics before the Lushan earthquake

Before the Wenchuan earthquake, all segments of the LFZ were in locked status with slow extrusion deformation backgrounds [4–6]. In particular, the rate of crustal deformation in the southern segment of the LFZ was higher than that of the middle-northern segment [7].

The Wenchuan earthquake unlocked the middle-northern segment of the LFZ, which accelerated the eastward movement of the eastern part of the Bayan Har block. As a result, the strain accumulation rate in the southern segment of the LFZ, which was still in locked status, obviously increased. The GPS velocities and strain-rate fields from 2009 to2011 are presented in Figure 2. The campaign GPS network was surveyed in 2009 and 2011, and for every station, one surveying section was surveyed for more than 3 days. The GPS velocity was processed using the GAMIT/GBLOBK software [8,9] and the QOCA software [10]. In this process, all observations for a given day, including 28 continuous stations from the TEONEC and 12 IGS stations, are combined to solve for the daily loosely constrained solutions of station coordinates and satellite orbits (Hfile) using the GAMIT software [8]. For a given day, the campaign stations, i.e. 14 continuous stations from the TEONEC and 7 IGS stations, are solved in the same manner. More than 100 continuous stations in a global distribution are combined and solved using the same strategy. Then, the daily solutions, including

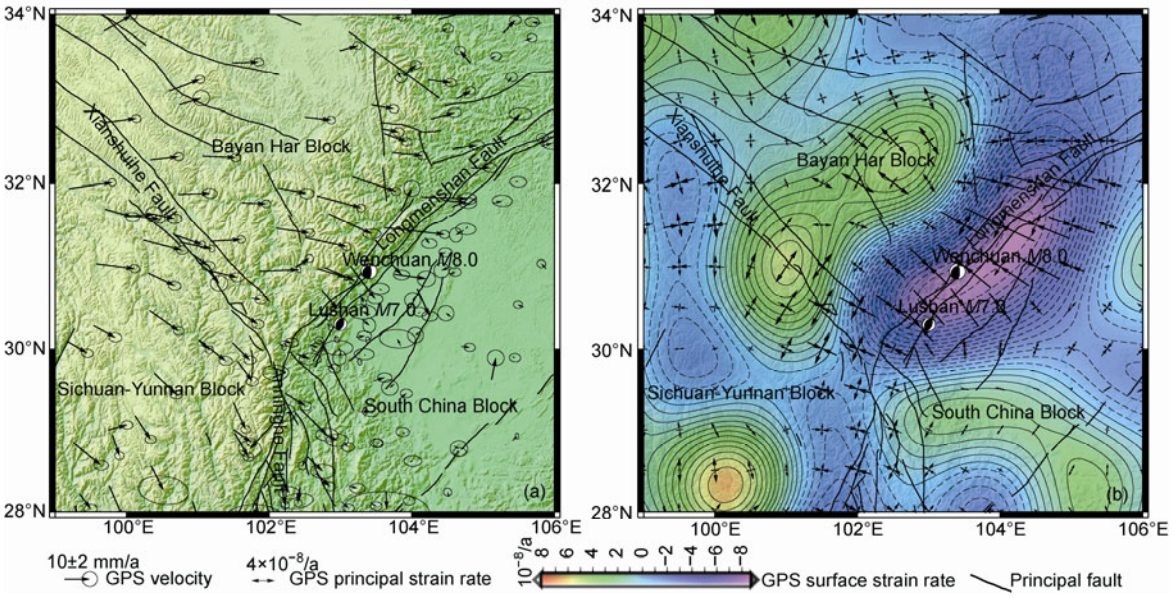

Figure 2 The GPS deformation field from 2009 to 2011. (a) GPS velocity field relative to the South China Block; (b) GPS strain-rate field.

many Hfiles, are combined to estimate the station coordinates and velocities in the ITRF2005 reference frame using the QOCA software [10], in which 85 stations in global distribution are used as frame points. Finally, the velocity solution is fixed to the South China Block reference [5]. The strain-rate field is calculated using the least-squares collocation method for a spherical surface [11,12]. The GPS velocity field relative to the South China block shows that the deformation mode can be separated by the epicenter of the Wenchuan earthquake into two different types (Figure 2(a)). The middle-northern segment of the LFZ is in post-seismic adjustment status because its northwestern side shows tension strain release features, but the southern segment is still in locked status because it shows continuous deformation characteristics that are different from the fault slip feature in the middle-northern segment. Considering that the strain- rate field presented in Figure 2(b) is obtained based on the continuous deformation hypothesis, the extrusion region in the middle-northern segment of the LFZ mainly results from the fault slip because we do not subtract the fault slip from the GPS velocity fields. As Figure 2(a) shows, the deformation in the southern segment of the LFZ has continuous characteristics, and the extrusion strain-rate distribution in this region, as reflected by Figure 2(b), shows accumulation features. Compared to the low level of strain accumulation suggested by previous publications [5,6], the rate of strain accumulation from 2009 to 2011 is remarkably faster than it was before the Wenchuan earthquake.

The middle-northern segment of the LFZ was in unlocked status after the Wenchuan earthquake, which accelerated the eastward movement of the eastern part of the Bayan Har block. The continuous GPS results in the southern segment of the LFZ illustrate that the crustal shortening rate is remarkably larger than before the Wenchuan earthquake and that the deformation is weakened in the hypocentral region of the Lushan earthquake.

3 Coseismic displacement of the Lushan M_S7.0 earthquake

We collect and process GPS continuous stations within 300 km of the epicenter from April 16, 2013, to April 23, 2013. The coseismic displacements of the Lushan M_S7.0 earthquake are presented in Figure 3. In this occupation and for all stations except LS04 and LS06, data were recorded for no less than 3 days before the earthquake and for the same duration after this event. These continuous GPS stations include the GPS network in the southern segment of the LFZ, the CORS GPS stations of the Earthquake Administration of Sichuan Province and some permanent GPS stations of the TEONEC that are located in the vicinity of the LFZ. The coseismic displacements are solved using the GAMIT/GLOBK software [8,9] with a strategy similar used in previous reports [13–15]. To obtain the precise satellite orbit and to realize the ITRF2008 reference, we process approximately 100 IGS stations in addition to the above 48 stations. In the solving process, we check the repeatability of the daily solutions first and then discard the unsteady stations and enlarge the error disturbances of individual stations with gross errors. Finally, we use the daily solutions, including station coordinates and their variance-covariance matrix, as quasi-observations to estimate the coordinates of all stations and the coseismic displacement of local stations.

(i) The range and magnitude of coseismic displacement distribution. The range of the coseismic displacement (detected by GPS surveys) is approximately 230 km (NW direction) × 100 km (SW direction), and the coseismic displacements that are larger than 10 mm are mainly located in a 100-km region (NW direction). The coseismic displacement significantly covers the whole southern segment of the LFZ. In particular, the LS07 (Qingjiang) station, which is located at the edge of the Wenchuan-Maowen fault, moves 30.0±1.1 mm in the SE direction, while the LS08 (Qiaoji) station, which is located approximately 18 km along the northwest side of the Wenchuan-Maowen fault, moves 10.8±1.5 mm. These results illustrate that the Lushan earthquake releases strain in the whole southern segment of the LFZ. Conversely, the coseismic displacement amplitude of the Lushan earthquake detected using GPS is not large. The displacement of the LS05 (Lushan) station, which is nearest to the epicenter, is maximal, and the horizontal component is 67.5 mm in the 188° direction, while the vertical component is 83.6 mm. The coseismic displacement of LS05 is preliminary technical result, and the steady analysis to this station will be tracked with the future surveying data.

(ii) Fault dislocation pattern reflected by the coseismic displacement field. The wide-ranging coseismic displacement distribution indicates that the thrust movement is dominant. The hanging wall (NW side of the fault) moves along the southeast direction, and the foot wall (SE side of the fault) moves to the northwest. However, the thrust values are remarkably small within the 70-km region close to the earthquake fault, and they do not correspond with the attenuation characteristics of strain release with increasing distance from the fault. Thus, we infer that any possible earthquake rupture does not reach the surface. Another possibility is that this phenomenon results from ruptures of more than one fault. Meanwhile, the laevorotation movements and strain release are remarkable in the 50-km region located in the hanging wall close to the earthquake fault. These results indicate that the thrust rupture is dominant and that the laevorotation movement is secondary with regard to the strain release of this earthquake. To quantitatively describe the laevorotation dislocation, we use a power function to fit the NE component of the coseismic displacement (the gray curve in Figure 4), in which the projection region is the dashed box in Figure 3. The fitting results illustrate that, assuming that the seismogenic fault rupture is located

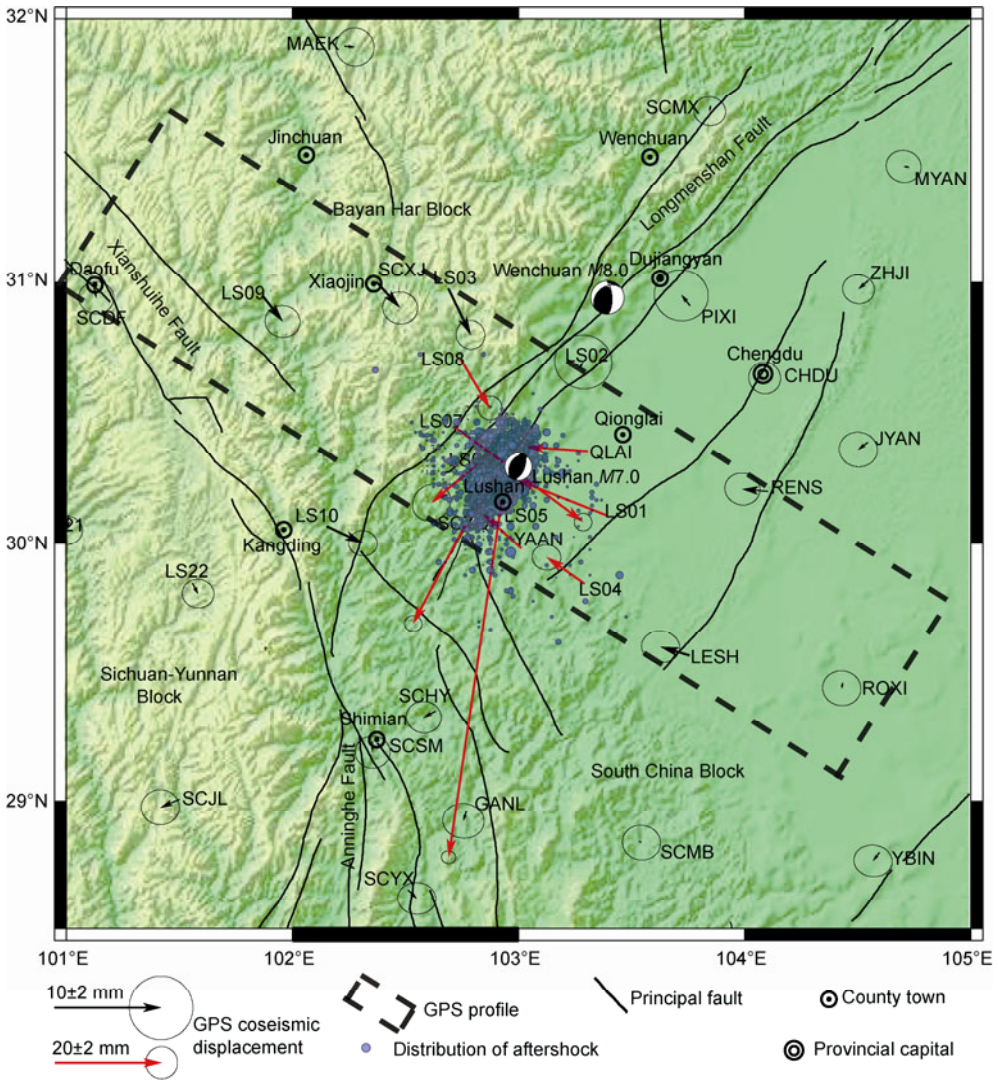

Figure 3 Coseismic horizontal displacement field of the Lushan M_S7.0 earthquake determined via GPS surveys (aftershocks records cutoff: 10 o'clock on May 12, 2013).

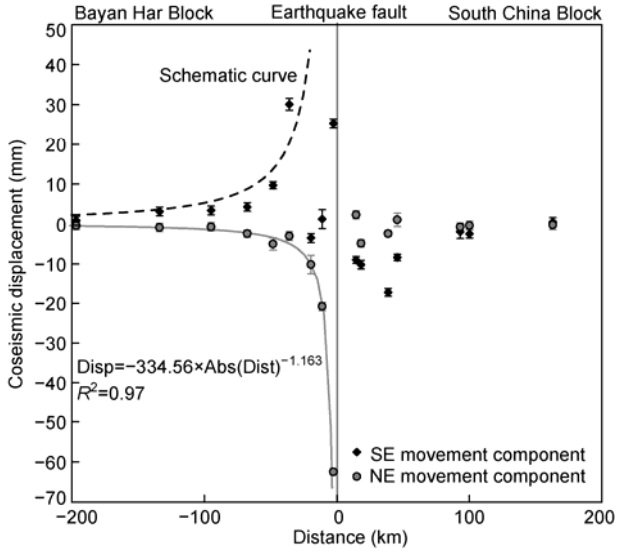

Figure 4 GPS profile results of horizontal displacement across the fault of the Lushan M_S7.0 earthquake.

to the east of the LS05 station by approximately 4 km, the power function can achieve a high degree of consistency with the coseismic displacement, thereby indicating that the laevorotation strain release is real.

The LS07 station (approximately 37 km from the seismogenic fault), which is located at the western edge of the Wenchuan-Maowen fault, shows a maximal thrust displacement in the horizontal component. The thrust component of the near-field station is significantly smaller than that of this horizontal component, which is inconsistent with the common observation that coseismic displacement decays with distance leaving the rupture zone. Therefore, the fitting curve cannot be obtained as a strike-slip component. According to the coseismic displacement distribution characteristics of the Wenchuan earthquake, we use a black dotted line to indicate the possible attenuation trend of the thrust coseismic displacement in Figure 4. If the earthquake rupture is completely exposed to the surface, the decay mode of the thrust component may be in accordance with

the characteristics of the dotted line in Figure 4. Based on this trend, we can infer that the thrust displacement is 3 times greater than the amount of sinistral displacement when the distance is 50 km from the seismogenic fault, and that a closer rupture zone results in a greater difference between the thrust and the strike-slip component. Considering the attenuation curves in Figure 4 and comparing the results of different coseismic displacement components, we can infer that the magnitude and scope of strain release in the direction perpendicular to the fault is much greater than that in the parallel direction.

(iii) Estimation of the location of the seismogenic fault based on the coseismic displacement. As the surface rupture is not found in wide scale, the seismogenic fault remains unclear after the earthquake. The LS05 station, located on the eastern side of the Guanxian-Anxian fault, records a maximum displacement of 83.6±3.7 mm in the uplift direction, while the vertical displacement of the LS06 station (located west of LS05) is 16.3±12.4 mm. All of the vertical displacements of the GPS stations located on the east side of LS05 are not obvious, and their horizontal displacements are mainly in the northwest direction (perpendicular to the fault). Thus, we can infer that the surface location of the seismogenic fault may be on the east of the LS05 station. Based on the coseismic displacement attenuation features shown in Figure 4, we estimate that the surface location of the earthquake fault is on the southeast side of the LS05 station by approximately 4 km. As a result, the seismogenic fault of the Lushan earthquake may be one fault to the east of the Guanxian-Anxian fault, which is close to the Chengdu Plain.

The attenuation of the coseismic displacement decays rapidly from LS05 to LS02 in the northeast direction. This finding indicates that the fault rupture does not connect with the rupture zone of the Wenchuan earthquake, which is supported by the aftershock distribution shown in Figure 3. Meanwhile, the station at which the maximum horizontal thrust displacement was recorded is located at the western edge of the Wenchuan-Maowen fault, indicating that the Lushan earthquake is associated with the deep detachment surface of the LFZ [4].

4 Discussion and conclusion

It may be possible to predict the location of the next strong earthquake using the coseismic displacement distribution of the huge Wenchuan earthquake. Subsequent monitoring of this possible earthquake fault has practical significance with regard to understanding the pregnancy and occurrence of the next strong earthquake. The surface coseismic displacement distribution of the Lushan earthquake has particularities. For example, the thrust rupture is dominant, while the laevorotation movement is secondary with regard to the strain release of this earthquake, a result that differs from the seismology inversion results. The range of the coseismic displacement distribution is large, but the amount of thrust is remarkably smaller near the fault. Thus, further discussion is beneficial for understanding the earthquake and its associated dynamics.

The surface coseismic displacement recorded via GPS surveys reveals that the seismogenic fault dislocation pattern is thrust with some amount of sinistral slip. However, the focal mechanism of the Lushan earthquake indicates that the rupture results entirely from thrust (http://www.globalcmt.org/, Liu et al. [16] and Zeng et al. [17]). To understand the differences between these two results, we first analyze the direction of the principal strain rate from 2009 to2011 (Figure 2(b)) and find that the direction of the principal tensile strain rate in the focal region is approximately 232±4°. The strike of the focal nodal plane presented by reference [16] is 214°, while the previously published value is 212° [17], which are consistent with the aftershock distribution. The angle between the principle tensile strain rate and the focal nodal plane is approximately 20°, corresponding to an angle between the principal compressional strain and the seismogenic fault strike of approximately 70°. Thus, it appears that the sinistral deformation background in the direction of the seismogenic fault existed before the Lushan earthquake. In addition, the focal mechanism equates to the rupture mode of the deep crust, while the GPS coseismic displacement reflects the surface dislocation mode. We present the following qualitative explanations for this difference. Because the rupture does not reach the surface, the near-surface crust remains in a high-stress state in the principal stress direction, which inhibits the thrust movement to a large degree. Conversely, shear movement occurs relatively easily in the direction parallel to the fault because the background horizontal stress is much lower than that in the principal stress direction. However, because of limitations in the data reported herein, the above laevorotation rupture in the crustal surface may result from the edge effect, in which the rupture does not reach the surface.

The displacement scope of the Lushan earthquake covers the whole southern segment of the LFZ, indicating that the strain release is not small. However, the coseismic displacement along the fault direction decays fast, and its range is small, indicating that the amount of strain release is limited. In addition, the GPS coseismic displacement and aftershock distribution indicate that the ruptures of the Lushan and Wenchuan earthquakes do not connect. As a result, the Lushan earthquake does not completely unlock the whole southern segment of the LFZ, so that continuous monitoring of the space-time process of crustal relative motion in this region is necessary to further understanding of the earthquakes' trends.

The thrust displacement that is near-field to the seismogenic fault is small, but the sinistral slip distribution is consistent with typical attenuation characteristics of coseismic displacement. To understand the mechanics of this earth-

quake and to determine the strain accumulation status after this shock in the southern segment of the LFZ, we should combine considerations of geological structure, crustal media characteristics and further observations in future studies.

Some GPS data are from Engineering Research Center of China Crust Movement Observation Network and the Earthquake Administration of Sichuan Province. The operation of the GPS temporary continuous network in the southern segment of the LFZ is under the support of the Surveying Engineering Institute of Earthquake Administration of Sichuan Province. Special thanks to Prof. Zhang P Z, Wen X Z, Tian Q J and Du F for their helpful advice. This work was supported by the National Key Technology R&D Program in the 12th Five-year Plan of China (2012BAK19B01), the National Natural Science Foundation of China (41274008 and 41104004), the Basic Research Project of Institute of Earthquake Science of China Earthquake Administration (2011IES010101), the Specific Fund of Seismic Industry of China Earthquake Administration (201008007) and the Scientific Investigation Projects of the Wenchuan and Lushan Earthquakes, CEA.

1 Xu X W, Han Z J, Li C Y, et al. Lushan M_S7.0 earthquake: A blind reserve-fault earthquake. Chin Sci Bull, 2013, 58: 3437–3443
2 Zhang Y, Xu L S, Chen Y T. Rupture process of the Lushan 4.20 earthquake and preliminary analysis on the disaster-causing mechanism (in Chinese). Chin J Geophys, 2013, 56: 1408–1411
3 Liao H, Xu R, Chen W F, et al. Property variation and statistical analysis of Sichuan GPS time series before and after Wenchuan Earthquake (in Chinese). Chin J Geophys, 2013, 56: 1237–1245
4 Zhang P Z, Xu X W, Wen X Z, et a1. Slip rates and recurrence intervals of the Longmen Shan active fault zone, and tectonic implications for the mechanism of the May 12 Wenchuan earthquake, 2008, Sichuan, China (in Chinese). Chin J Geophys, 2008, 51: 1066–1073
5 Jiang Z S, Fang Y, Wu Y Q, et al. The dynamic process of regional crustal movement and deformation before Wenchuan M_S8.0 earthquake (in Chinese). Chin J Geophys, 2009, 52: 505–518
6 Li Y X, Zhang J H, Zhou W, et al. The mechanism and dynamics of the generation and occurrence for Wenchuan M_S8.0 earthquake (in Chinese). Chin J Geophys, 2009, 52: 519–530
7 Wu Y Q, Jiang Z S, Yang G H, et al. Evolution characteristics of strain rate field reflected by GPS data before Wenchuan earthqake (in Chinese). J Geod Geodyn, 2011, 31: 20–25
8 Herring T A, King R W, McClusky S C. GAMIT Reference Manual. GPS Analysis at MIT. Release 10.4. Massachussetts Institute Technology, http://www-gpsg.mit.edu/~simon/gtgk/index.htm (last accessed 2011 October 5), 2010
9 Herring T A, King R W, McClusky S C. GLOBK Reference Manual. Global Kalman filter VLBI and GPS analysis program. Release 10.4. Massachussetts Institute Technology, http://www-gpsg.mit.edu/~simon/gtgk/index.htm (last accessed 2011 October 5), 2010
10 Dong D, Hering T A, King R W. Estimating regional deformation from a combination of space and terrestrial geodetic data. J Geophys Res, 1998, 72: 200–214
11 Wu Y Q, Jiang Z S, Yang G H, et al. The application and method of GPS strain calculation in whole mode using least-squares collocation in sphere surface (in Chinese). Chin J Geophys, 2009, 52: 1707–1711
12 Wu Y Q, Jiang Z S, Yang G H, et al. Comparison of GPS strain rate computing methods and their reliability. Geophys J Int, 2011, 185: 703–717
13 Niu Z, Wang M, Sun H, et al. Contemporary velocity field of crustal movement of Chinese mainland from Global Positioning System measurements. Chin Sci Bull, 2005, 50: 839–840
14 Wang M, Zhang P, Shen Z. Far-filed coseismic surface displacement of Sumatra earthquake in Indonesia by global positional system (GPS) measurement. Chin Sci Bull, 2006, 51: 365–368
15 Working Group of the Crustal Motion Observation Network of China Project. Coseismic displacement field of the 2008 M_S8.0 Wenchuan earthquake determined by GPS (in Chinese). Sci China Earth Sci, 2008, 38: 1195–1206
16 Liu J, Yi G X, Zhang Z W, et al. Introduction to the Lushan, Sichuan *M*7.0 earthquake on 20 April 2013 (in Chinese). Chin J Geophys, 2013, 56: 1404–1407
17 Zeng X F, Luo Y, Han L B, et al. The Lushan M_S7.0 earthquake on 20 April 2013: A high-angle thrust event (in Chinese). Chin J Geophys, 2013, 56: 1418–1424